Blue Silica Nanoparticles Based Colorimetric Immunoassay for detection of Salmonella pullorum

Article *in* Analytical methods · August 2015
DOI: 10.1039/C5AY02073E

3 authors, including:

Wenchao Dou
Zhejiang Gongshang University
33 PUBLICATIONS **373** CITATIONS

SEE PROFILE

Analytical Methods

PAPER

Cite this: *Anal. Methods*, 2015, **7**, 8647

Blue silica nanoparticle-based colorimetric immunoassay for detection of *Salmonella pullorum*

Qian Sun, Guangying Zhao and Wenchao Dou*

A colorimetric immunoassay based on blue silica nanoparticles (blue-SiNPs) was developed for quantitative detection of *Salmonella pullorum* (*S. pullorum*). In this method, blue-SiNPs were synthesized by doping C.I. reactive blue 21 into silica nanoparticles using a reverse microemulsion method. Blue-SiNPs functionalized with anti-*S. pullorum* were employed as detection probes. Magnetic nanoparticles (MNPs), employed as supports for the immobilization of polyclonal antibodies against *S. pullorum*, were used as capture probes. The sandwich structures of MNP-*S. pullorum*-blue-SiNPs were separated with a magnet and etched with NaOH. The C.I. reactive blue 21, released from silica nanoparticles, was used as a colorimetric indicator. The absorbance of C.I. reactive blue 21 at 675 nm is proportional to the concentration of *S. pullorum*. Under optimal conditions, the developed colorimetric immunoassay exhibited a wide dynamic range of 4.4×10^2 CFU mL^{-1} to 4.4×10^7 CFU mL^{-1} toward *S. pullorum* with a detection limit of 4.4×10^1 CFU mL^{-1}. For application of the assay, this method is not influenced by the complex matrix of practical samples. The recoveries of *S. pullorum* from chicken liver samples were from 94.5% to 108% with a good correlation coefficient ($R^2 = 0.9989$) with those obtained by an official standard culture method. We also show that this colorimetric immunoassay can be carried out on a microplate reader with a 96-well plate. This method is particularly economic, simple, rapid, specific and has good stability. The new technology provided a basis for the detection of other pathogenic bacteria and viruses. Such a simple colorimetric immunoassay holds great potential as an on-site tool for clinical diagnosis of bacteria and viruses.

Received 7th August 2015
Accepted 9th August 2015

DOI: 10.1039/c5ay02073e

www.rsc.org/methods

Introduction

Conventional bacterial testing methods involve several basic steps: pre-enrichment, selective enrichment, selective plating, and biochemical screening and serological confirmation.[1] Culture medium preparation, inoculation of plates and colony counting make these methods labor-intensive and time-consuming, and it may take several days before the results are obtained.[2] There are increasing demands for the rapid and reliable detection of food-borne pathogens. The advent of biotechnology has greatly altered pathogenic bacterial testing methods. Colorimetric immunoassay is one of the widely used techniques among all assay techniques, taking advantage of the antigen–antibody reaction and color changes to identify a substance.[3] It has gained great attention in various research areas including food safety, clinical diagnosis and environmental monitoring.[4,5] In comparison with fluorescence-based assays, the colorimetric immunoassay has significant advantages of low cost without the requirement of fluorescent-labeled antibodies and expensive instruments.[6] Colorimetric immunoassays can be used for on-site detection with a portable UV-Vis absorption spectrometer.

Transforming the detection event into a color change is a key technology of colorimetric immunoassays, which is very crucial for obtaining low detection limits.[7–9] Enzyme-labeled nanoparticles and gold nanoparticles are commonly exploited as signal transduction tools in colorimetric immunoassays.[10,11] The carried enzyme molecule enters and participates in the catalytic reaction, and the high efficiency of enzymes makes them especially suitable for ultrasensitive bioanalysis. However, short lifetime, high price and critical operating situations limit enzyme immunoassay applicability.[12] In recent years, the great superiority of gold nanoparticles in colorimetric immunoassays has been reported. Gold nanoparticles have been used in colorimetric immunoassays to enhance the stability, improve sensitivity, or simplify the manipulation process. The color and absorption spectrum of gold nanoparticles shift to longer wavelengths if aggregation occurs. However, the absorption intensity of gold nanoparticles is substantially affected by various factors such as pH, temperature, and salt concentration.[13,14] Furthermore, it is not economical to use gold nanoparticles for the routine detection of bacteria in foods. As the reported assay is imperfect, we aim to develop a colorimetric immunoassay for pathogenic bacterial detection, which has the

Food Safety Key Laboratory of Zhejiang Province, School of Food Science and Biotechnology, Zhejiang Gongshang University, Hangzhou 310018, China. E-mail: wdou@zjsu.edu.cn

potential to fulfill the WHO ASSURED criteria (affordable, sensitive, specific, user-friendly, robust and rapid, equipment free, and deliverable to those who need them).

In addition to the above-mentioned nanoparticles, silica nanoparticles (SiNPs) are widely used in several fields including disease labeling, drug delivery and biosensing.[15] But most reported SiNPs are white or colorless, and they are not suitable for signal conversion and signal amplification.[16] Organic dyes have rich color and good stability, and do not fade under the harsh conditions of light, heat, acid, alkali and so on. From a chemical point of view, so many kinds of organic dyes and their good chemical reactivity make them very suitable for dyeing silica nanoparticles to synthesis colored silica nanoparticles. Colored silica nanoparticles are good candidates for use as optical labels in biotechnological systems due to their inherent advantages, such as bright color, easy preparation and good biocompatibility.[17,18] In our previous work, we had developed an agglutination test for simultaneous detection of two different pathogenic bacteria using the colored silica nanoparticles as carriers.[19]

Practical samples are highly complex consisting of fats, proteins, minerals and even sometimes contain antimicrobial preservatives. In order to discriminate the target pathogen from the complex matrix, a separation step is normally required. Further, they are numerically very low, so efficient pathogen separation and concentration techniques need to be developed for specific detection of pathogens and to avoid false-negative results.[20] Magnetic nanomaterials, due to their unique properties including being conveniently manipulated by a magnet, high surface to volume ratio, and fast kinetics in solution, have been widely applied for rapid, efficient, and specific capture and enrichment of target bacteria from the original samples.[21,22] For example, Pang's group had successfully used antibody-modified magnetic nanomaterials to capture *Salmonella typhimurium* at ultralow concentration ($\sim$10 CFU mL^{-1}).[23] On the other hand, magnetic capture can easily be coupled with many detection methods, such as colorimetric immunoassay, PCR, fluorescence observation, and electrochemical immunosensing. When MNPs are applied to colorimetric immunoassays, the assay is usually fast and simple to operate, which offers a promising platform for the detection of various analytes.[24]

The aim of this work is to exploit a blue silica nanoparticle (blue-SiNP) and magnetic nanoparticle (MNP) based colorimetric immunoassay for the rapid detection of pathogenic bacteria. In this study, *Salmonella pullorum* (*S. pullorum*) was used as a model analyte. In most developed nations, *S. pullorum* is a common infectious pathogen and can result in acute systemic diseases and a high incidence of mortality in young poultry.[25] Rapid and sensitive detection of *S. pullorum* is of great importance for poultry breeding. Aimed at making a stable color indicator for a sandwich immunoassay, we chose an organic dye (C.I. reactive blue 21) to synthesize the blue-SiNPs using an inverse microemulsion method. Organic dyes were modified to the surface of SiNPs with a silane coupling agent. Herein, magnetic nanoparticles (MNPs) and blue-SiNPs were modified with antibodies to construct antibody-coated magnetic nanoparticles (IgG-MNPs) and antibody-coated blue-SiNPs (IgG-blue-SiNPs), respectively. The IgG-MNPs were used for enrichment and separation of *S. pullorum*. The IgG-blue-SiNPs, which encapsulated hundreds of C.I. reactive blue 21 into a single nanosphere, were employed as reporter probes to provide a highly amplified and stable signal. After adding sodium hydroxide in the detection solution, blue-SiNPs generate a colorimetric signal that is directly proportional to the concentration of *S. pullorum*.

Experimental section

Materials and instruments

A variety of bacteria were employed in this work including *S. pullorum* as the target bacteria, and *Bacillus subtilis* (*B. subtilis*), *Escherichia coli* (*E. coli*), *Staphylococcus aureus* (*S. aureus*), *Enterobacter sakazakii* (*E. sakazakii*) as the control group. All bacteria were conserved in the laboratory of the authors. *S. pullorum* was grown at 37 °C in a lysogeny broth (LB) medium with shaking. Cells were harvested in the late exponential growth phase by centrifugation and washed in triplicate using physiological saline aqueous solution. Concentration of the bacteria was confirmed by colony counting (CFU mL^{-1}). The enriched bacteria were inactivated with 0.5% formaldehyde and stored at 4 °C before use.

Triton X-100, cyclohexane, hexanol, glutaraldehyde (GLU, 50 wt%) and ammonia (25–28 wt%) were obtained from Chengdu Kelong Chemical Reagent Co., Ltd (Chengdu, China). 3-[2-(2-Aminoethylamino)ethylamino]propyl-trimethoxysilane (APTMS) and tetraethyl orthosilicate (TEOS) were obtained from Aladdin Industrial Inc. (Shanghai, China). Bovine serum albumin (BSA) was obtained from Beijing Dingguo Biotechnolgy Co. Ltd (Beijing, China). Magnetic nanoparticles (Prot Elut NHS, 100–120 nm, MNPs) were obtained from Enriching Biotechnology Ltd (Shanghai, China). C.I. reactive blue 21 was supplied by Zhejiang Shunlong Chemical Co., Ltd (Zhejiang, China). Polyclonal antibody against *S. pullorum* (100 μg mL^{-1}) was purchased from China Institute of Veterinary Drug Control (Beijing, China). Other reagents were all of analytical grade and were used as received without further purification. The water used was doubly distilled.

A Hitachi SU-70 scanning electron microscope (SEM) was purchased from Hitachi Inc. (Tokyo, Japan). The Malvern Nano 2S potential laser particle analyzer was provided by Malvern Instruments Co., Ltd (Worcestershire, UK.). The Thermo Nicolet 380 Fourier transform infrared (FTIR) spectrometer (Shanghai, China). The SpectraMax 190 microplate reader was purchased from Molecular Devices (Orleans, USA). The 3–18 K high speed refrigerated centrifuge was purchased from Sigma Laborzentrifugen GmbH (Osterode, Germany). The Scientz-09 pat type sterile homogenizer was provided by NingBo Scientz Biotechnology Co., Ltd (Ningbo, China). All electrochemical experiments were performed at room temperature (25 ± 1 °C).

Synthesis of blue-SiNPs and blue-SiNP-NH_2

Synthesis of blue-SiNPs was carried out according to the method described by a previous paper with a little change.[26] The

details of the procedure are described as follows. The water-in-oil (W/O) microemulsion was prepared at room temperature first by mixing 2 mL surfactant Trition X-100, 8 mL oil phase cyclohexane and 2 mL cosurfactant *n*-hexanol. 0.15 mL C.I. reactive blue 21 solution (100 mg mL^{-1}) and 400 μL of water were then added. Then the resulting mixtures were homogenized with magnetic force stirring for 15 min to form a W/O microemulsion. In the presence of 100 μL of TEOS and 20 μL of APTMS, a hydrolyzation reaction was initiated by adding 100 μL of $NH_3 \cdot H_2O$ (25–28 wt%) under stirring. The reaction was allowed to stir for 48 h. After the reaction was completed, acetone was added to break the microemulsion and recover the particles. The contents were then centrifuged and washed with ethanol and water several times to remove surfactant molecules and physically adsorbed C.I. reactive blue 21 from the particles' surface. The synthesized blue-SiNPs were characterized by SEM.

30 mg of blue-SiNPs were ultrasonically resuspended in the mixed solution of 15 mL ethanol and 40 μL APTMS and it was allowed to complete the silanized reaction under stirring overnight at room temperature. After this reaction, amino groups were introduced to the surface of blue-SiNPs. Amino-modified blue-SiNPs (blue-SiNPs-NH_2) were isolated by centrifugation at 8000 rpm and washed three times with 0.01 M phosphate buffered saline solution (PBS, pH 7.3). The synthesized blue-SiNPs and blue-SiNP-NH_2 were characterized by FTIR, zeta potential and by SEM.

Surface functionalization of nanoparticles

Covalent immobilization of the antibody onto the functionalized blue-SiNP surface. The polyclonal antibody against *S. pullorum* was directly immobilized onto the functionalized blue-SiNPs by the well-established glutaraldehyde method.[27,28] The immobilization protocols were the following (Fig. 1): (1) 20 mg of blue-SiNP-NH_2 was dispersed into 5 mL PBS (0.01 M, pH 7.3) buffer containing 2.5% glutaraldehyde for about 3 h; (2) the nanoparticles were separated by centrifugation and washed with PBS three times. After the nanoparticles re-dispersed in PBS, they were further incubated with the anti-*S. pullorum* polyclonal antibody for 2 h at room temperature with shaking; (3) the antibody-coupled blue-SiNPs (IgG-blue-SiNPs) were centrifuged at 8500 rpm and washed with PBS several times to remove the excess antibody and kept at 4 °C in PBS (0.01 M, pH 7.3) for its following use.

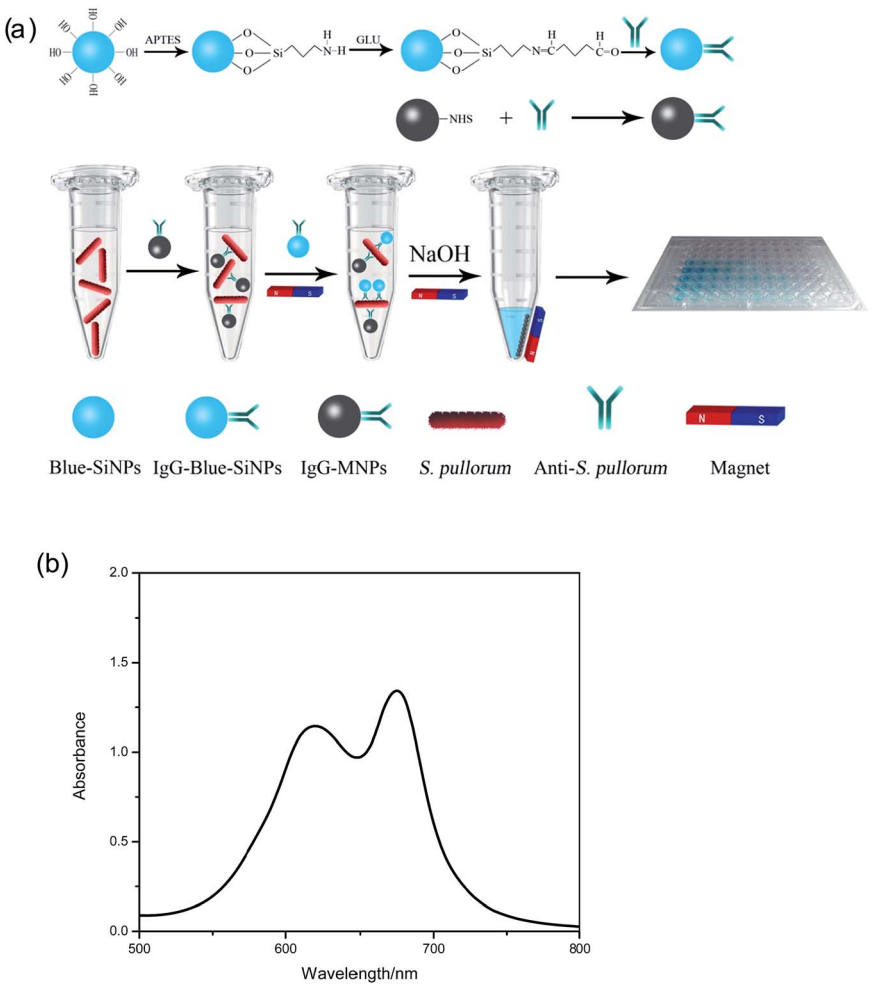

Fig. 1 (a) Schematic view of the colorimetric immunoassay for rapid detection of *S. pullorum* and *S. gallinarum* based on blue-SiNPs and MNPs. (b) The UV-Vis spectra of the C.I. reactive blue 21.

Preparation of IgG-MNPs. The polyclonal antibody against *S. pullorum* was covalently conjugated to carboxyl-modified MNPs according to the manufacturer's instructions. 100 μL of magnetic nanoparticles (10 mg mL^{-1}) were mixed with 50 μL of the antibody against *S. pullorum*. The reaction was allowed to proceed at 4 °C overnight. The mixture was washed for three times with a washing buffer in a magnetic field. Unreacted active groups on the MNPs were blocked with 1% BSA. Finally, the antibody modified magnetic nanoparticles (IgG-MNPs) were dispersed in 1 mL of PBS and stored at 4 °C before use.

Procedures of colorimetric immunoassay measurement. The colorimetric immunoassay was carried out as follows: 20 μL IgG-MNPs (1 mg mL^{-1}) were mixed with 1 mL *S. pullorum* solution in a centrifuge tube. After incubating for 30 min at 37 °C with gentle shaking, the resulting mixture was separated magnetically and washed with PBS for three times to remove any unbound species. The immune complexes of IgG-MNPs and *S. pullorum* were then dispersed in 20 μL PBS. 20 μL IgG-blue SiNPs (10 mg mL^{-1}) were added into the mixture and allowed to react for 15 min. IgG-blue SiNPs and IgG-MNPs formed sandwich structures with *S. pullorum via* immune reaction. The final sandwich immune complexes were washed by PBS to remove unbound IgG-blue SiNPs. The final sandwich immune complexes were incubated with 50 μL of NaOH aqueous solutions (5 mol L^{-1}) for 15–60 min. After the C.I. reactive blue 21 was desorbed, the supernatants including C.I. reactive blue 21 were separated and transferred to a 96-well plate. The absorbance of C.I. reactive blue 21 was measured with a microplate reader at 675 nm.

Results and discussion

Characterization of blue-SiNPs

An inverse microemulsion method was chosen to prepare blue-SiNPs in this study. The inverse microemulsion method is a simple and diverse preparation method for synthesis of silica nanoparticles in the laboratory, and it is easy to control the morphology of silica nanoparticles. The physical image of blue-SiNPs showed that they were bright in color and highly dispersible in aqueous solution (Fig. 2 inset). The size and morphology of blue-SiNPs were characterized by SEM (Fig. 2). The nanoparticles had excellent monodispersibility and all blue-SiNPs showed a spherical shape and smooth surface. The average diameters of the nanoparticles determined by SEM were approximately 45 ± 5 nm and the size distribution was also quite uniform and the characteristics of colored-SiNPs were in accordance with the descriptions by Tan *et al.*[29]

The presence of a chemical group on the outermost layer of blue-SiNPs was confirmed by zeta potential determination. zeta-potential measurement was carried out using a Zetasizer. For the determination of the zeta potential, pH of samples was adjusted by addition of 0.01 M HCl or 0.01 M NaOH. All values shown in this work were an average of three measurements. Fig. 3a displays the zeta potential of blue-SiNPs and blue-SiNP-NH_2 as a function of pH. The isoelectric point (IEP) of blue-SiNPs is at pH 4.8. When blue-SiNPs are in the environment of a neutral solution, the surface potential of blue-SiNPs is about −13 mV, which indicates that the blue-SiNP surface has a

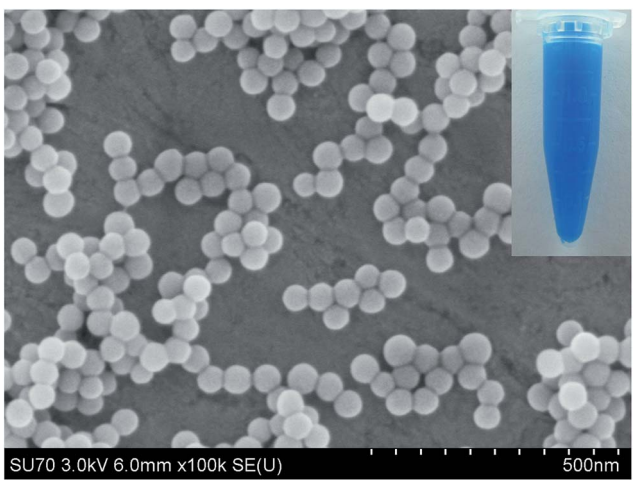

Fig. 2 The SEM image of blue-SiNp and the physical image of the blue-SiNp (inset).

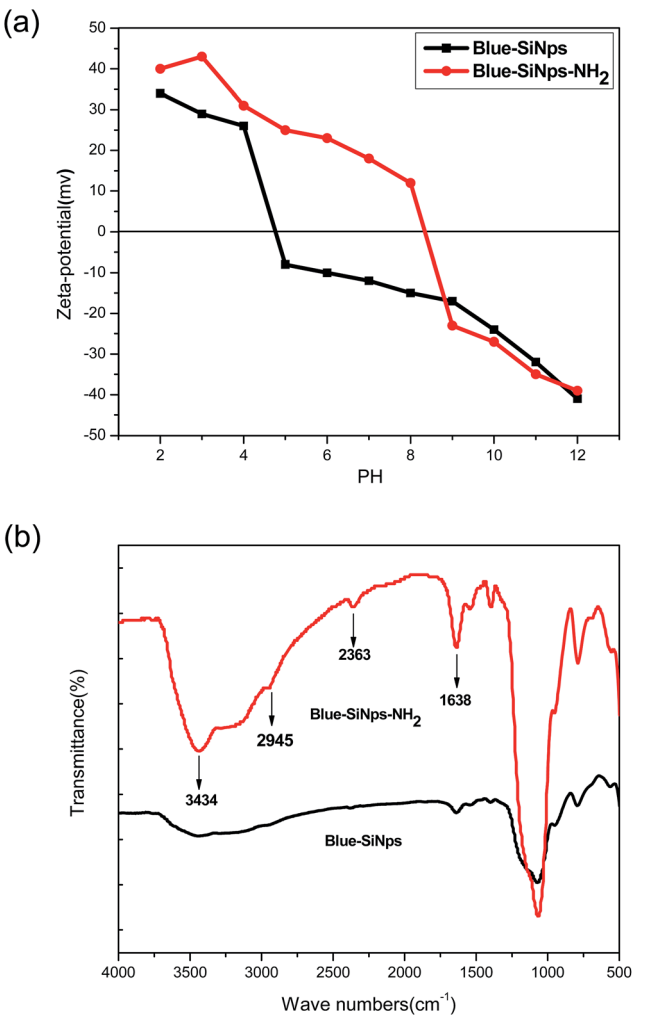

Fig. 3 (a) Zeta potential of blue-SiNPs (bottom) and blue-SiNP-NH_2 (top). (b) FTIR spectra of blue-SiNPs (bottom) and blue-SiNP-NH_2 (top).

negative charge, because of the presence of hydroxyl groups; the IEP of blue-SiNPs-NH_2 is shifted to pH 9.5, and in neutral solution, the surface potential of blue-SiNPs-NH_2 is about 18 mV, which indicates that the blue-SiNP-NH_2 surface has a positive charge. The increase of the zeta potential is attributed to the increasing number of protonated amine groups on the blue-SiNP-NH_2 surface.

FT-IR analysis provides a direct proof for the amine fictionalization. Chemical compositions on the surface of blue-SiNPs and blue-SiNPs-NH_2 were examined by FTIR (Fig. 3b). Dried samples were measured using the KBr pellet method in the range of 400–4000 cm^{-1}. A strong IR absorption band at the region 980–1220 cm^{-1}, corresponding to the Si–O–Si of the silica core, is found in both blue-SiNPs and blue-SiNP-NH_2. A new band at 2945 cm^{-1} in the blue-SiNP-NH_2 is assigned to the N–H of the silica. Compared to blue-SiNPs, the absorption spectra of blue-SiNP-NH_2 have a significant difference in the region 2900–3450 cm^{-1}. These results are consistent with the blue-SiNPs being successfully coated with an aminated silica shell. APTMS is thus believed to have been successfully introduced onto the surface of the silica modified nanoparticles.

Principle of the blue-SiNP-based colorimetric assay for the detection of *S. pullorum*

The principle of the blue-SiNP-based colorimetric assay for the detection of *S. pullorum* is presented in Fig. 1. We use the colorimetric immunoassay to detect *S. pullorum* based on blue-SiNPs and MNPs. In a typical assay, blue-SiNP probes and MMP formed a sandwich structure with the target *S. pullorum* according to the principle of antigen–antibody binding. A magnetic field was used to effectively remove unbound blue-SiNP probes. In order to quantify the amount of *S. pullorum*, desorption experiments were carried out. The NaOH aqueous solution (5 mol L^{-1}) was used for the release of the loaded C.I. reactive blue 21 by etching blue-SiNPs. There was a correspondence between the absorbance of C.I. reactive blue 21 and the *S. pullorum* concentration. By measuring the absorbance, we could quantitatively determine the concentration of *S. pullorum* in the sample. Meanwhile, we could also qualitatively determine the *S. pullorum* level by the change in visible color. As shown in Fig. 1b, the spectrum of C.I. reactive blue 21 exhibited a strong absorption peak at 675 nm. In order to sensitively quantify the amount of *S. pullorum*, we measured the absorbance of C.I. reactive blue 21 at 675 nm for establishing a standard curve between the absorbance and the amount of *S. pullorum*.

Optimization of experimental conditions

To achieve an optimal analytical performance, the experimental conditions for the blue-SiNP-based colorimetric system were further optimized through adjusting incubation times of IgG-MNPs with *S. pullorum* from 0 to 60 min and the IgG-MNP concentration from 0.25 to 4 mg mL^{-1}. The performance of the developed colorimetric immunoassay could be greatly affected by incubation times. Fig. 4a shows the absorbance changes of C.I. reactive blue 21 with different incubation times, the absorbance rapidly increased with the increasing incubation

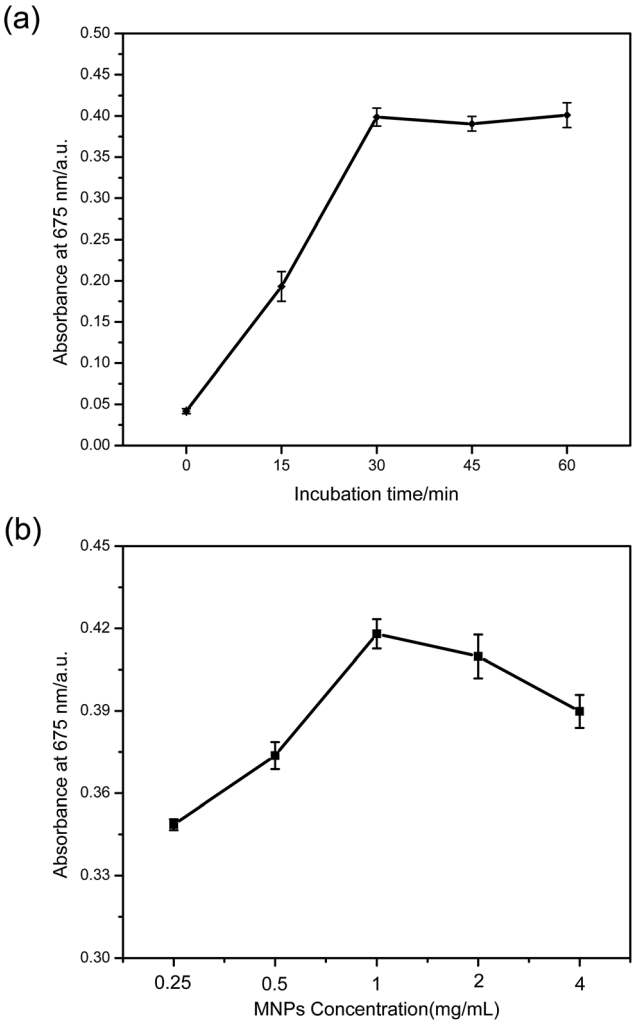

Fig. 4 The effects of (a) incubation time and (b) MNP concentration on the absorbance intensity of C.I. reactive blue 21.

time, which indicates that *S. pullorum* gradually binds with the magnetic beads *via* antigen–antibody reaction. And a maximum was attained at 30 min. A further increase in the incubation time, *e.g.* 40 min, had very little additional beneficial effects. Besides the limited diffusion of IgG-MNPs, a 30-min incubation was chosen in this study.

The concentration of IgG-MNPs in the detection system was optimized by using 20 μL IgG-MNPs of different concentrations from 0.25 to 4 mg mL^{-1}. As seen from Fig. 4b, the absorbance increased with the increasing concentration of IgG-MNPs until it reached 1 mg mL^{-1}, and the absorbance tended to level off when the concentration is higher than 1 mg mL^{-1}. In the condition of 1 mg mL^{-1}, IgG-MNPs could combine with the suitable concentration of *S. pullorum*. Therefore, 1 mg mL^{-1} was chosen as the optimal concentration of IgG-MNPs for detection of *S. pullorum* in the following experiment.

Sensitivity of the colorimetric immunoassay

Under optimal experimental conditions, we examined the performance of the proposed immunoassay with different

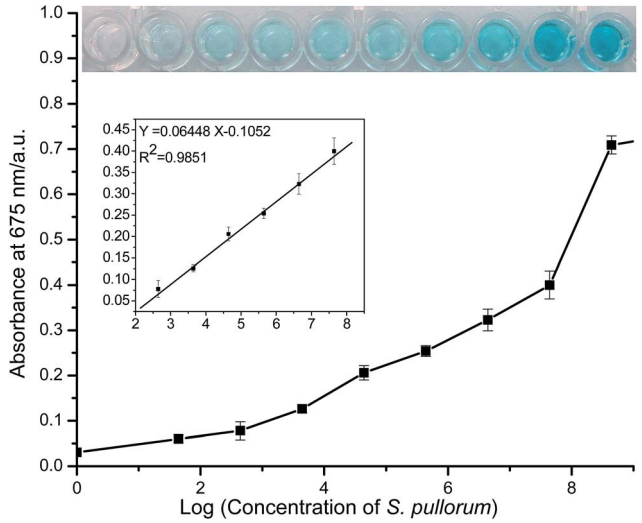

Fig. 5 The linear relationship of absorbance intensity *versus* the logarithm of *S. pullorum* concentrations under optimal conditions (insets: the corresponding photographs of the C.I. reactive blue 21 in a 96-well plate (up); the linear correlation of absorbance intensities *versus* logarithm of *S. pullorum* concentrations (down)).

concentrations of *S. pullorum* in the range from 4.4×10^1 to 4.4×10^9 CFU mL^{-1}. The plot of the absorbance of C.I. reactive blue 21 *versus* the logarithm of *S. pullorum* concentration is shown in Fig. 5 inset (down). According to the results of absorbance measurements, a linear dependence between the absorbance and the logarithm of *S. pullorum* concentration was obtained in the range from 4.4×10^2 to 4.4×10^7 CFU mL^{-1}. The linear regression equation was $y = 0.06448 \log x - 0.1052$ ($R^2 = 0.9851$). The *S. pullorum* concentration in the samples was obtained quantitatively *via* the linear regression equation. The limit of detection (LOD) was 4.4×10^1 CFU mL^{-1}, defined as 3SD above the zero-dose response ($n = 10$). This was comparable with those of other nanolabel-based immunoassays for pathogenic bacteria. The sensitivity of the classic ELISA reported by Dainty and Cudjoe was 10^5 CFU mL^{-1} for *Salmonella*.[30] The higher sensitivity exhibited by the blue-SiNP-based immunoassay was attributed to using the blue-SiNP as a signal amplifier. Each blue-SiNP could accumulate thousands of C.I. reactive blue 21 molecules owing to its high surface-to-volume ratio. Thus one immunoreaction event could bring multiple C.I. reactive blue 21 molecules, leading to the large amplification of signals.

The analytical performance of the proposed immunosensor was compared with that of other pathogenic bacteria sandwich immunosensors reported (Table 1). The comparison suggests superior analytical performance of the present immunosensor over some previously reported sandwich immunosensors. The fluorescent immunosensor reported by Pang *et al.* was an exception.[23] They used a fluorescence microscope that leads to four times of magnitude improvement insensitivity for bacterial detection, but the technology was more complicated and the time that was needed for the process was longer. Magalhaes *et al.* had also reported a more sensitive method than this work, however, the linear range of their method was poor; it could not be used for quantitative detection of *Salmonella typhimurium*.

Specificity of the blue SiNP-based colorimetric assay

The selection of an antibody with a high specificity is important in developing an immunoassay, because the specificity for the measurement of analytes in all immunoassay systems is dependent on the antibody used.[10] In this study, a commercial antibody to *S. pullorum* was used. The specificity of the developed colorimetric method was evaluated with five control experiments that involved *B. subtilis*, *E. coli*, *S. aureus*, *E. sakazakii* and PBS, respectively. Equal concentrations of *S. pullorum*, *B. subtilis*, *E. coli*, *S. aureus* and *E. sakazakii* were detected with the same colorimetric immunoassay as mentioned in Section 2.5. After incubation and separation, the colorimetric assay displayed both an obvious blue color (inset in Fig. 6) and a strong increase in the absorbance at 675 nm (as showed in Fig. 6) in the presence of *S. pullorum*. In contrast, there was neither blue color (inset in Fig. 6) nor strong absorbance (Fig. 6) observed in the presence of *B. subtilis*, *E. coli*, *S. aureus* and *E. sakazakii* as compared with the PBS without bacteria. These results indicated the high specificity of the proposed method for the detection of *S. pullorum*.

Applicability of the assay

To evaluate the detection capability and reliability of the developed colorimetric immunoassay in practical samples,

Table 1 Comparison of the present work with other sandwich immunosensors for the determination of pathogenic bacteria using MNPs[a]

Detection method	Materials	Analytical ranges (cfu mL^{-1})	LODs (CFU mL^{-1})	Ref.
SV	Copper-AuNPs	1.30×10^2 to 2.6×10^3	98.9	32
Potentiometric assay	QDs	None	20	33
Chemiluminescence	HRP + luminol + H_2O_2	None	2.6×10^5	34
Fluorescence	QDs	2.5×10^3 to 1.95×10^8	500	35
Fluorescence	IFNS	10^3 to 10^5	10	23
Absorbance	TiO_2 nanocrystals	10^2 to 10^8	>100	14
Absorbance	Peroxidase + ABTS	10^5 to 10^7	10^5	30
Absorbance	Blue-SiNPs	4.4×10^2 to 4.4×10^7	4.4×10^1	Ours

[a] SV: stripping voltammetry, QDs: quantum dots, AuNPs: gold nanoparticles, HRP: horseradish peroxidase, IFNS: immunofluorescent nanospheres, and ABTS: 2′-azinobis-(3-ethylbenzothiazoline-6-sulfonate).

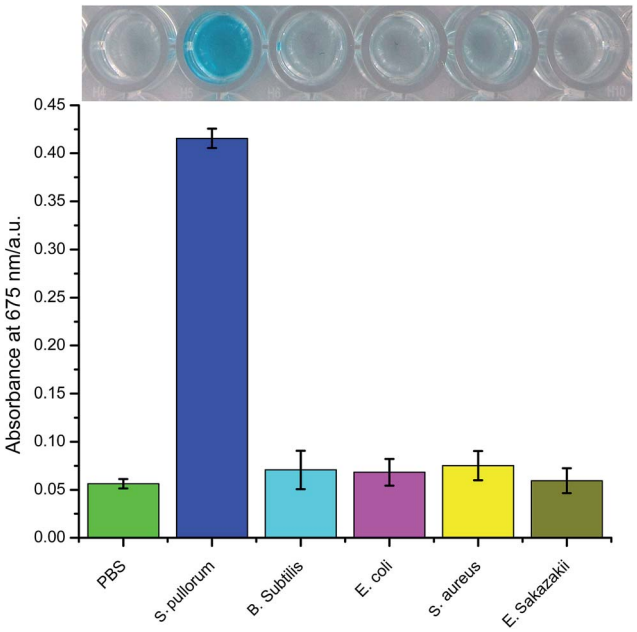

Fig. 6 Specificity of the colorimetric immunoassay, from left to right: PBS (0.01 mol mL^{-1}), *S. pullorum* (10^7 CFU mL^{-1}), *B. subtilis* (10^7 CFU mL^{-1}), *E. coli* (10^7 CFU mL^{-1}), *S. aureus* (10^7 CFU mL^{-1}), and *E. sakazakii* (10^7 CFU mL^{-1}) (insets: the corresponding photographs).

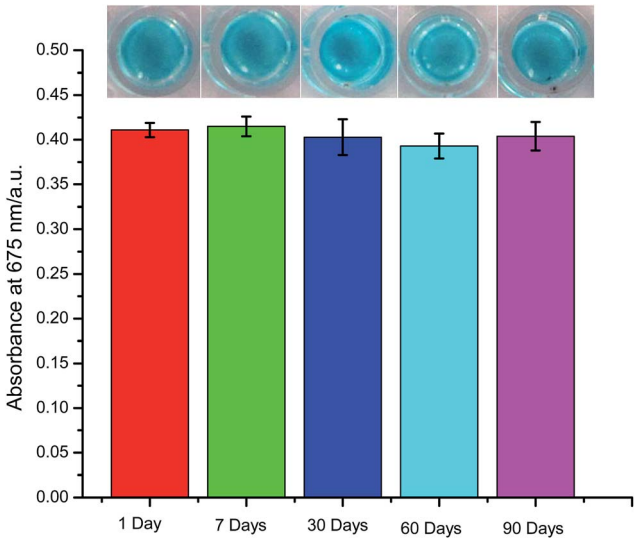

Fig. 7 Stability of the colorimetric immunoassay after IgG-MNPs and IgG-blue-SiNPs were stored for: 1 day, 7 days, 30 days, 60 days, and 90 days (insets: the corresponding photographs).

commercial chicken livers were used to make artificially contaminated samples. Chicken livers were collected from a local supermarket in Hangzhou (Zhejiang, China), and they were homogenized by a pat type sterile homogenizer. The chicken livers were seeded with serial dilutions of *S. pullorum* to achieve a final concentration from 4.4×10^2 to 4.4×10^7. The recoveries and CVs of the above-mentioned samples spiked with different concentrations of *S. pullorum* are listed in Table 2. With a simple and rapid detection procedure using the colorimetric immunoassay, most of the recoveries of *S. pullorum* for these samples were 101%, 94.5%, 95.0%, 104.9%, 102%, and 108%, respectively. All the recoveries were in the range from 90 to 110%. The correlation coefficient (R^2) of the results obtained from the colorimetric immunoassay was 0.9989. Conventional microbiological methods based on the standard plate count are time-consuming for the identification and quantification of *S. pullorum*. The colorimetric immunoassay established in this study is based on the specific induction of the blue-SiNPs, resulting in an absorbance change in a dose dependent manner. This assay, which is of high sensitivity and capable of quantitatively recognizing *S. pullorum*, is more sophisticated and specific than the conventional microbiological method. Further, this method is easy to perform and is suitable for detection of *S. pullorum* in practical samples such as animal tissues.

Table 2 The assay results for the commercial chicken liver infected by different concentrations of *S. pullorum* by using the developed colorimetric immunoassay

Samples	Added (CFU mL^{-1})	Detected (CFU mL^{-1})	Recovery (%)
1	4.4×10^2	4.44×10^2	101
2	4.4×10^3	4.34×10^3	94.5
3	4.4×10^4	4.19×10^4	95.0
4	4.4×10^5	4.50×10^5	104.9
5	4.4×10^6	4.47×10^6	102
6	4.4×10^7	4.77×10^7	108

Stability

The long-term stability of IgG-blue-SiNPs and IgG-MNPs was examined. Their stabilities were studied by detecting *S. pullorum* with the developed colorimetric immunoassay after IgG-MNPs and IgG-blue-SiNPs were stored at 4 °C for 1, 7, 30, 60 and 90 days. As shown in Fig. 7, during a three-month test, the absorbance of the organic dye was almost unchanged for the 90 days' measurement. So these two kinds of immune nanoparticles were found to be able to retain similar reaction activity after storage at 4 °C for at least 90 days. Actually, the thus-prepared colorimetric immunoassay is more stable compared with biosensors based on enzyme-coated nanoparticles.[31] We speculate that the long-term stability is mainly attributed to the following two issues: (i) the enzyme labeled antibody was replaced by the antibody to modify the blue-SiNPs, and (ii) anti-*S. pullorum* molecules were covalently immobilized on the surface of the blue-SiNPs and MNPs.

Conclusions

In conclusion, this work demonstrates the development of an advanced colorimetric immunoassay based on IgG-blue-SiNPs for the detection of *S. pullorum*. Although blue SiNPs were synthesized with inexpensive commercial organic dyes and TEOS, they were excellent markers for colorimetric immunoassays. Another important innovation present in this paper is the demonstration that the blue-SiNP-based assays can be

carried out in a 96-well plate, thus meeting the demands of high-throughput analysis. We show that the direct quantitation of *S. pullorum* by measuring the absorbance of the organic dye is an easy, fast, and reliable way to quantify the total bacteria. For application of the assay, this method is not influenced by the complex matrix of practical samples and has good sensitivity. Compared with the conventional colorimetric immunoassay system, highlights of this work mainly are as follows: IgG-blue-SiNPs were used for loading the anti-*S. pullorum* polyclonal antibody and used as the signal amplification probe, we can directly take advantage of the absorbance of the organic dye modified in the surface of SiNPs to quantify the bacteria; this developed colorimetric immunoassay method does not need the catalysis of enzymes to make it more economical and can be applied in more detection places; this method has high selectivity and sensitivity, it could effectively discriminate *S. pullorum* from other four pathogenic bacteria, besides, the detection limit is 4.4×10^1 CFU mL^{-1}, which is much lower than the detection limit of 10^4 CFU mL^{-1} of the conventional colorimetric immunoassay to detect salmonella. Furthermore, the blue silica nanoparticle- and magnetic nanoparticle-based colorimetric immunoassay method does not require sophisticated instruments and is well suitable for other pathogenic microorganisms or even investigated for rapid detection of viruses.

Acknowledgements

This project was supported by the Food Science and Engineering, the most important discipline of Zhejiang province (ZYTSP20141062) and the analysis and testing projects of the Zhejiang public innovation platform (2015C37023).

References

1 S. Koyuncu, M. G. Andersson and P. Haggblom, *Appl. Environ. Microbiol.*, 2010, **76**, 2815.
2 X. Ye, Y. Wang and X. Lin, *Curr. Microbiol.*, 2011, **63**, 477.
3 Y. Song, W. Wei and X. Qu, *Adv. Mater.*, 2011, **23**, 4215.
4 Z. Gao, M. Xu, L. Hou, G. Chen and D. Tang, *Anal. Chem.*, 2013, **85**, 6945.
5 A. M. López Marzo, J. Pons, D. A. Blake and A. Merkoçi, *Anal. Chem.*, 2013, **85**, 3532.
6 W. Qu, Y. Liu, D. Liu, Z. Wang and X. Jiang, *Angew. Chem.*, 2011, **123**, 3504.
7 Z. Gao, M. Xu, M. Lu, G. Chen and D. Tang, *Biosens. Bioelectron.*, 2015, **70**, 194.
8 M. Liu, C. Jia, Q. Jin, X. Lou, S. Yao, J. Xiang and J. Zhao, *Talanta*, 2010, **81**, 1625.
9 A. Lesniewski, M. Los, M. Jonsson-Niedziółka, A. Krajewska, K. Szot, J. M. Los and J. Niedziolka-Jonsson, *Bioconjugate Chem.*, 2014, **25**, 644.
10 H.-S. Kim and B.-K. Oh, *BioChip J.*, 2014, **8**, 1.
11 X. Wang, L. Wu, J. Ren, D. Miyoshi, N. Sugimoto and X. Qu, *Biosens. Bioelectron.*, 2011, **26**, 4804.
12 H.-H. Yang, S.-Q. Zhang, X.-L. Chen, Z.-X. Zhuang, J.-G. Xu and X.-R. Wang, *Anal. Chem.*, 2004, **76**, 1316.
13 J. J. Storhoff, R. Elghanian, R. C. Mucic, C. A. Mirkin and R. L. Letsinger, *J. Am. Chem. Soc.*, 1998, **120**, 1959.
14 J. Joo, C. Yim, D. Kwon, J. Lee, H. H. Shin, H. J. Cha and S. Jeon, *Analyst*, 2012, **137**, 3609.
15 R. P. Bagwe, C. Yang, L. R. Hilliard and W. Tan, *Langmuir*, 2004, **20**, 8336.
16 R. P. Bagwe, L. R. Hilliard and W. Tan, *Langmuir*, 2006, **22**, 4357.
17 F. M. Winnik, B. Keoshkerian, J. Roderick Fuller and P. G. Hofstra, *Dyes Pigm.*, 1990, **14**, 101.
18 H. Giesche and E. Matijević, *Dyes Pigm.*, 1991, **17**, 323.
19 H. Yu, G. Zhao and W. Dou, *Curr. Pharm. Biotechnol.*, 2015, **16**, 716.
20 T. Asahara, T. Murohara, A. Sullivan, M. Silver, R. van der Zee, T. Li, B. Witzenbichler, G. Schatteman and J. M. Isner, *Science*, 1997, **275**, 964.
21 Y. Zhang, C. Pilapong, Y. Guo, Z. Ling, O. Cespedes, P. Quirke and D. Zhou, *Anal. Chem.*, 2013, **85**, 9238.
22 Y. Zhao, M. Ye, Q. Chao, N. Jia, Y. Ge and H. Shen, *J. Agric. Food Chem.*, 2009, **57**, 517.
23 C.-Y. Wen, J. Hu, Z.-L. Zhang, Z.-Q. Tian, G.-P. Ou, Y.-L. Liao, Y. Li, M. Xie, Z.-Y. Sun and D.-W. Pang, *Anal. Chem.*, 2013, **85**, 1223.
24 M. Liang, K. Fan, Y. Pan, H. Jiang, F. Wang, D. Yang, D. Lu, J. Feng, J. Zhao, L. Yang and X. Yan, *Anal. Chem.*, 2013, **85**, 308.
25 R. K. Gast, *Poult. Sci.*, 1997, **76**, 17.
26 R. P. Bagwe, C. Yang, L. R. Hilliard and W. Tan, *Langmuir*, 2004, **20**, 8336.
27 I. Willner and E. Katz, *Angew. Chem., Int. Ed.*, 2000, **39**, 1180.
28 M. V. Kiselev, A. K. Gladilin, N. S. Melik-Nubarov, P. G. Sveshnikov, P. Miethe and A. V. Levashov, *Anal. Biochem.*, 1999, **269**, 393.
29 X. Zhao, R. Tapec-Dytioco and W. Tan, *J. Am. Chem. Soc.*, 2003, **125**, 11474.
30 K. S. Cudjoe, T. Hagtvedt and R. Dainty, *Int. J. Food Microbiol.*, 1995, **27**, 11.
31 D. Tang, B. Su, J. Tang, J. Ren and G. Chen, *Anal. Chem.*, 2010, **82**, 1527.
32 W. Dungchai, W. Siangproh, W. Chaicumpa, P. Tongtawe and O. Chailapakul, *Talanta*, 2008, **77**, 727.
33 N. F. D. Silva, J. M. C. S. Magalhaes, M. T. Oliva-Teles and C. Delerue-Matos, *Anal. Methods*, 2015, **7**, 4008.
34 G. Pappert, M. Rieger, R. Niessner and M. Seidel, *Microchim. Acta*, 2010, **168**, 1.
35 H. Kuang, G. Cui, X. Chen, H. Yin, Q. Yong, L. Xu, C. Peng, L. Wang and C. Xu, *Int. J. Mol. Sci.*, 2013, **14**, 8603.